DOI: 10.1002/ejic.201000634

Silicon Nanowires – Synthesis, Properties, and Applications

Mingwang Shao,*[a] Dorthy Duo Duo Ma,[b] and Shuit-Tong Lee*[b]

Keywords: Silicon / Nanostructures / Heterogeneous catalysis / Imaging agents / Sensors

In this review, we summarize the essential aspects of the synthesis, properties, and applications of silicon nanowires. In particular, important applications such as catalysis, Li ion batteries, solar cells, biological and chemical sensors are discussed.

Introduction

Nanowires are an important class of one-dimensional (1D) materials that have been attracting a great deal of interest recently. 1D nanomaterials, especially of semiconductors, usually exhibit unique and superior electronic, optical, mechanical, thermal, and chemical properties, and are actively investigated for basic science and for technological applications ranging from chemical, biological and environmental sensors and field-effect transistors to logic circuits. Silicon nanowires (SiNWs) are one of the most important 1D semiconductors,[1,2] partly due to their ready implementation in modern industry in established processes. SiNWs are expected to play a key role in applications such as solar cells, sensors, lithium batteries, and catalysts with regard to their surface-dependent properties. In this article, we review the current status of SiNWs research, especially the synthesis, properties, and applications of these materials.

[a] Institute of Functional Nano & Soft Materials (FUNSOM) and Jiangsu Key Laboratory for Carbon-Based Functional Materials & Devices, Soochow University,
Suzhou, Jiangsu 215123, China
Fax: 86-512-65882846
E-mail: mwshao@suda.edu.cn
[b] Center of Super-Diamond and Advanced Films and Department of Physics and Materials Science,
City University of Hong Kong, Hong Kong SAR, China
E-mail: apannale@cityu.edu.hk

Mingwang Shao is a Professor at the Institute of Functional Nano & Soft Materials (FUNSOM) and the Jiangsu Key Laboratory for Carbon-Based Functional Materials & Devices, Soochow University, P.R. China. His research interests include inorganic solid materials, biological and chemical sensors.

Dorothy Duo Duo Ma is a Senior Engineer at the Center of Super-Diamond and Advanced Films (COSDAF), City University of Hong Kong, Hong Kong SAR. Her research interests include nanoscience and nanotechnology, scanning probe microscopy.

Shuit-Tong Lee is a member of the Chinese Academy of Sciences and a Fellow of TWAS (the Academy of Sciences for the Developing World). He is currently Chair Professor of Materials Science and Director of the Center of Super-Diamond and Advanced Films (COSDAF), City University of Hong Kong, Hong Kong SAR, and Director of the Institute of Functional Nano & Soft Materials (FUNSOM) and the Jiangsu Key Laboratory for Carbon-Based Functional Materials & Devices, Soochow University, P.R. China. His research interests include nanomaterials and nanotechnology, organic electronics, diamond and super hard materials, and surface science.

1. Synthesis of SiNWs

A great deal of effort has been invested in preparing SiNWs for various applications. Numerous ways have been developed to synthesize SiNWs, including both the bottom-up and the top-down approaches. Several commonly used growth methods are described.

1.1. Vapor-Liquid-Solid (VLS) Growth

The classical chemical vapor deposition (CVD) method by a metal-catalytic vapor-liquid-solid (MC-VLS) mechanism is one of the most popular methods used to synthesize SiNWs.[3] In the MC-VLS process, a volatile gaseous silicon precursor, such as silane (SiH_4) or silicon tetrachloride ($SiCl_4$), serves as the silicon source. A metal capable of forming a low-temperature eutectic phase with Si is used as a catalyst for the growth of SiNWs.[4] When the Si-containing vapor passes over the metal catalyst heated to a temperature higher than the eutectic temperature of the metal–silicon system (363 °C for Au/Si and 156.6 °C for In/Si),[5] the vapor decomposes on the surface of the catalyst, and Si diffuses into the metal, forming a liquid metal/Si alloy. Upon reaching supersaturation, a SiNW then precipitates from the melt, the liquid alloy droplet remaining at the tip of the nanowire as it grows in length.[4,6]

CVD allows epitaxial growth of SiNWs, while the wire diameter and growth rate are affected by the initial size of the metal catalyst,[5,7] the growth temperature, and the type of Si precursor used. Using gold colloid seeding in the VLS-CVD method, Hochbaum et al. obtained SiNWs with some control of the diameter and density of vertical wires in selected regions.[8] To broaden the range of metal catalysts and lower the substrate temperature, plasma-enhanced CVD has been used for growing SiNWs.[9–12]

Gold is the most popular metallic catalyst used for growing SiNWs by the VLS mechanism. However, such CVD-VLS growth results in gold contamination, which induces deep-level electronic states in the band gap of Si and degrades the minority-carrier lifetime and diffusion length in SiNWs. Moreover, gold or metallic catalysts are undesirable for complementary metal oxide semiconductors (CMOSs). Therefore, more benign metals, which are less detrimental to the minority-carrier lifetime and more compatible with CMOS, such as copper and aluminum, are preferred. Indeed, metal catalysts, such as Cu,[13] Sn,[14] In,[14] Ga,[15] and Al,[16] have been used in the VLS growth of SiNWs.

Generally speaking, MC-VLS as a bottom-up synthesis method offers better control of wire diameter[5] and patterning[17] of SiNWs, but affords a relatively low yield of production.

1.2. Thermal Evaporation Oxide-Assisted Growth (OAG)

The synthesis of SiNWs by the disproportionation of thermally evaporated SiO with or without the assistance of catalyst is a simple, efficient, and large-scale fabrication method.[18]

The yield and growth rate of SiNWs by this method is higher in a closed deposition system without circulation of inert carrier gas, but decreases with increasing ambient gas pressure. A lower pressure not only enhances the yield of SiNWs, but also ensures a smooth surface of the SiNWs.[19] The size, shape, and structure of SiNWs depend sensitively on their composition, as well as the temperature and other parameters of the synthetic process.[20]

Lee et al.[20,21] proposed an oxide-assisted mechanism for this method (Figure 1). Different metal catalysts for this growth method were studied.[22,23] SiNWs produced without metal catalyst are quite uniform and have average core diameters of about 20 nm.[2,24–28] Zeolite can be used as a template/precursor to grow very fine and uniform SiNWs by thermal evaporation. The wire diameter thus obtained can be as small as 1–5 nm.[29,30]

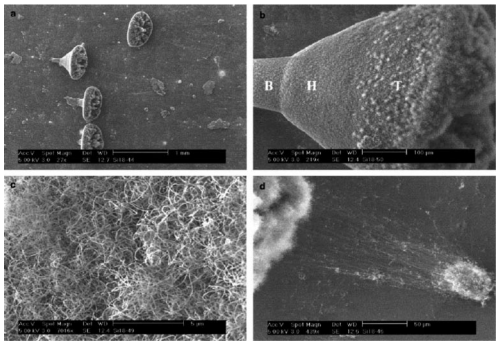

Figure 1. (a) SiNWs covered mushroom-shaped SiO particles deposited at 1180 °C, (b) a mushroom-shaped particle, (c) SiNWs on the smooth cone surface of a mushroom-shaped particle, and (d) many straight and parallel SiNWs connecting a mushroom-shaped particle and another particle nearby (possibly a piece broken off from the former). Reprinted with permission from ref.[20]

For various applications, SiNWs of different morphologies,[31] doped by nitrogen[18] and as yarns,[32] can be synthesized by this method. The OAG method may be combined with VLS to obtain SiNWs with oscillation in diameter.[33]

1.3. Laser Ablation

The laser ablation technique at high temperature is an earlier method used to synthesize SiNWs.[1,27,34] In this process, a target made of (metal + Si) or (SiO_2 + Si) is heated in a furnace to about 1200 °C and then ablated by a laser beam. Inert gas is used as a carrier gas, which transports and cools the ablated products downstream where they are deposited as nanowires.[20]

The advantage is that SiNWs can be synthesized in high purity, high yield, and large quantity by this high-temperature laser evaporation method. The fast growth rate and the uniformly smooth curving feature of the nanowires are significantly different from the stiff whiskers grown from the vapor-liquid-solid mechanism.[35] Yet, the need of low-wavelength, high-energy, focused pulsed lasers prevents the method from having wide application.

The diameters of SiNWs synthesized by laser ablation vary significantly in different ambient gases such as He, Ar + H_2, and N_2[36] (Figure 2). The SiNWs synthesized in He and Ar (5% H_2) consist almost entirely of nanowires (Figure 2a and 2b), while some spherical particles composed of a mixture of crystalline Si and amorphous Si oxide are found to coexist with SiNWs grown in a N_2 atmosphere.

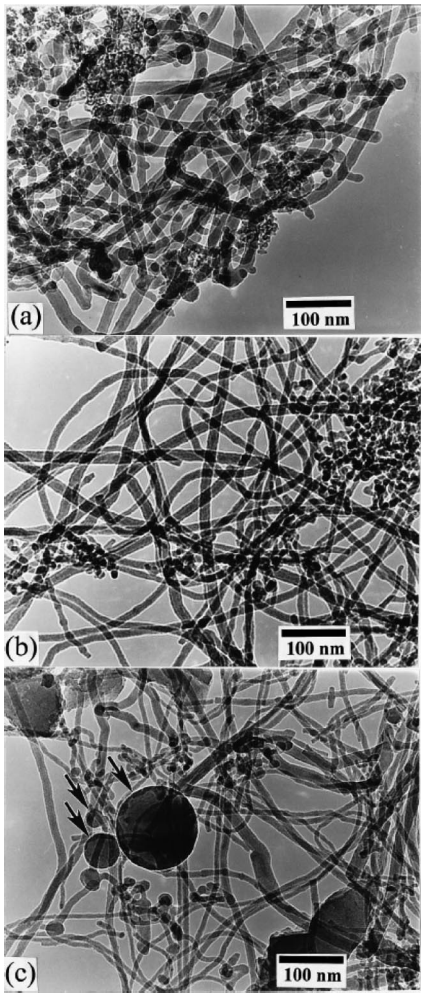

Figure 2. TEM micrographs of SINWs taken from typical samples of laser ablated products using different carrying gases: (a) He, (b) Ar (5% H_2), and (c) N_2. Reprinted with permission from ref.[36]

1.4. Chemical Etching

Chemical etching is a convenient technique for rapid fabrication of large-area, highly oriented SiNW arrays on Si wafers by metal-induced chemical etching of silicon substrates in HF solution near room temperature. The morphologies of the obtained microstructures on the surface of Si substrates are strongly affected by the parameters such as the etching temperature, solution concentration,[37] immersion time in the HF solution, the space between metal particles,[38,39] and, especially, the metal species added into the HF solution. The most widely used metals are Ag^+ and Au^+. Fe^{3+} may also be employed in this method.[40] SiNWs with higher density may be produced in a two-step process: that is, Ag deposition followed by etching in H_2O_2/HF.[41]

This etching method shows little dependence on the orientation or doping type of the Si wafer[38] and has the advantages of simplicity, large scale production, and low cost. However, it is hard to control the wire diameter and interspacing because of the random distribution of metal particles formed by electroless deposition or vacuum thermal evaporation. Peng et al. reported a simple extension of this method for the fabrication of SiNWs aligned in order, with desirable diameter, density, and doping characteristics, by depositing metals onto colloidal crystal templates.[42] Huang et al. reported a catalytic templated etching process to control the diameter, length, and density of SiNWs.[43] To understand the mechanisms of metal-induced etching and contamination, Peng et al. formulated an electrokinetic model, which satisfactorily explains the microscopic dynamic origin of the motility of metal particles in Si.[44]

1.5. Solution-Phase Synthesis

Korgel et al. used solution-phase synthesis to fabricate SiNWs in liquid media.[45] In this method, highly pressurized supercritical organic fluids enriched with a liquid Si precursor (such as diphenylsilane) and metal (Au or Ni) catalyst particles were utilized to synthesize SiNWs at temperatures above the metal-Si eutectic temperature. The Si precursor decomposed, and Si formed an alloy with the metal. Then a SiNW was precipitated from the alloy droplet once the alloy became supersaturated with Si. This process follows a supercritical-fluid-liquid-solid mechanism. Defect-free SiNWs with a nearly uniform diameter (as low as 4–5 nm) were fabricated by using this approach. Au,[45,46] Cu,[47] and Ni[48] nanocrystal catalysts can be used as seeds to direct 1D Si crystallization in a solvent heated and pressurized above its respective critical point. The orientation of the SiNWs could be controlled by monitoring the reaction pressure.[45] The wire growth kinetics influences nanowire morphology significantly and can be controlled effectively by using a supercritical fluid flow reactor.[46] Recently, Korgel et al. reported a solution-liquid-solid colloidal synthetic route carried out in an organic solvent (instead of a supercritical liquid) at atmospheric pressure that yielded crystalline SiNWs in large quantities with inexpensive equipment.[49]

1.6. Molecular Beam Epitaxy (MBE)

Synthesis of SiNWs by the MBE technique usually needs a high-purity solid Si source heated and crystallized under ultrahigh vacuum with Au as seed:[50–56] for example, SiNWs were produced by MBE (111)-oriented on Si (111) substrates. Similar to CVD, MBE was initially designed for epitaxial layer-by-layer deposition.[57] Yet, metal contamination was found to cause silicon wire growth in this case. The growth behavior differs essentially from the classical VLS mechanism for the growth of SiNWs by CVD. The

difference lies in the role of the metal seed, the wire morphology, and the aspect ratio. In particular, surface diffusion, including the metal used as well as Si, strongly influences the growth process.[52] From a thermodynamic point of view, the driving force for nanowire growth by MBE is related to the supersaturation determined by relaxation of elastic energy generated in the Si substrate due to Au intrusion.[54]

Although ordered arrays of vertically aligned SiNWs have been synthesized by MBE using prepatterned arrays of gold droplets (produced by nanosphere lithography) on Si(111) substrates,[51] problems still remain. For example, only nanowires with diameters greater than about 40 nm can be obtained,[52] and the growth rate is slow.[55]

1.7. Kármán Vortex Street Assisted Patterning Growth

Kármán vortex street assisted patterning growth was reported by Shao et al. to grow nanomaterial arrays as shown in Figure 3. In this method, a Kármán vortex street was employed to pattern catalysts and to grow nanomaterial arrays, which were made of a disk-like superstructure built of SiNWs. There were also nanowires connected with the disks.[58]

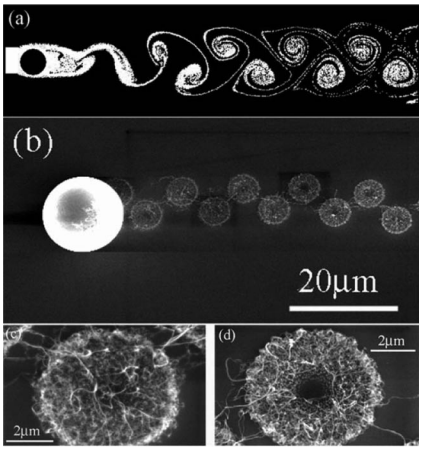

Figure 3. Image of a Kármán vortex street: (a) schematic diagram of a Kármán vortex street: there exists a wake between two adjacent vortices; (b) SEM image of a SiNW array with the form of a Kármán vortex street in addition to the preplaced tin particles; (c, d) single SiNW disks and SiNWs connected to the disks are clearly seen. Reprinted with permission from ref.[58]

In addition to the above methods, less common techniques have also been used to synthesize SiNWs, such as annealing in a reactive atmosphere,[59] hydrothermal growth,[60,61] and electric-field-assisted growth.[62]

Different synthetic methods yield SiNWs of different characteristics. MC-VLS and OAG are two common methods widely used to fabricate SiNWs, with their respective merits and shortcomings. The MC-VLS method provides better control of diameter and patterning of SiNWs but relatively low yield of production, and it uses difficult-to-handle raw materials. The OAG method can produce SiNWs in large quantities and without metal contamination, but with less control in wire pattern and diameter. The chemical etching technique (top-down fabrication) can readily produce large-area, highly oriented SiNW arrays, although of large size distribution, on Si wafers near room temperature. Single-crystal SiNWs with controlled diameters can be prepared by laser-assisted catalytic growth and molecular beam epitaxy employing expensive equipment. The axial orientation of SiNWs can be tuned by using the supercritical-fluid-liquid-solid method at mild temperature with the help of catalysts. Kármán vortex street assisted patterning growth might be employed in the research on transport properties of SiNWs. For specific applications, selection of the synthetic method needs to take into consideration the desired characteristics of each method.

2. Properties of SiNWs

In general, the properties of materials depend on their intrinsic structure. However, due to their small size, properties of nanomaterials are dominated by their surface properties. Consequently, SiNWs possess various distinctive features;[63] remarkably they can undergo n-i-p conduction changes in transport characteristics upon exposure to environments of different pH; such surface-dependent transport properties are significant for nanodevice design.[63]

2.1. Surface-Dependent Transport Properties

The conductance of SiNWs fabricated by chemical etching of a p-type Si wafer is substantially different in air from that of the original wafer, in that it increases with decreasing wire diameter. Field-effect transistors (FETs) fabricated from a SiNW show a hole concentration two orders of magnitude higher than that of the original wafer[63] from which the SiNW was etched. In vacuum, the conductivity of SiNWs dramatically decreases, whereas the hole mobility increases. Device performances are further improved by embedding SiNW FETs in SiO_2, which insulates the device from the atmosphere and passivates the surface defects of the NWs. Owing to the dominant surface effects, n-type SiNWs can even change and start to exhibit p-type characteristics. This phenomenon demonstrates that surface states can dominate the transport properties of SiNWs and that appropriate surface passivation can significantly improve the performance of SiNW FETs[64] (Figure 4).

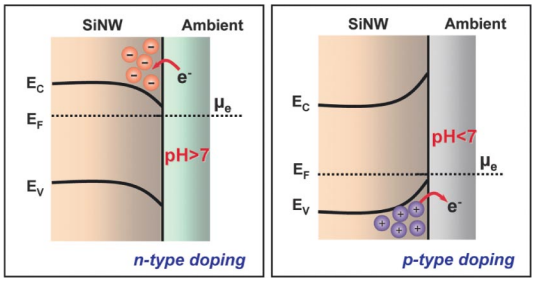

Figure 4. Schematic of band bending in SiNWs under n- and p-type doping by electron transfer at the interface between the SiNW and the wet layer. Reprinted with permission from ref.[64]

The tunable and reversible transition of p^+-p-i-n-n^+ conductance was demonstrated in nominally intrinsic SiNWs by simply changing surface conditions. SiNWs may be described as core-shell structures because of their large surface-to-volume ratio, and controlling the surface or shell in the core-shell model represents a universal way to tune the properties of the nanostructures.[64]

First-principle calculations confirmed the doping effects of SiNWs by surface passivation and adsorbates. The large surface-to-volume ratio of SiNWs provides high-efficiency surface modification. Surface effects allow effective doping of SiNWs by electron transfer across the surface layer, which provides a considerable concentration of majority carriers in SiNWs with surface passivating agents such as hydrogen.[65]

Surface-dominated properties, although observed in SiNWs, are expected to be common to other nanostructures of which the surface constitutes a significant portion. For example, the conductivity of undoped Ge nanowires is mainly due to surface state-induced hole accumulation.[66] Significantly, it suggests that modification of surfaces can potentially be a powerful approach to control the transport properties of nanostructures.

2.2. Chemical Reactions and Biomodification

Hydrogen-terminated SiNWs reacted with organic solvents, such as $CHCl_3$, CH_2Cl_2, or CH_3I, to produce hydrocarbon nanotubes and hydrocarbon nano-onions by bath sonication for 15 min under ambient conditions.[67,68] Hydrogen-terminated SiNWs were remarkably stable in air with a stability better than that of a Si wafer.[69] However, in protonated solution, H-SiNWs show moderate reactivity and may reduce noble metal ions[70,71] or noble metal alloys[72,73] (Figure 5) such as Pd, Rh,[74] and Ag.[75] H-SiNWs may reduce Hg^{2+} and react with 2,2,2-trifluoroethyl acrylate by a coupling route.[73]

The band gap of SiNWs may be modified by the use of different species for surface termination. The functional group used to saturate the silicon surface can significantly modify the band gap, resulting in corresponding energy shifts.[76] Moreover, the electronic properties of SiNWs may vary with molecular functional groups.[77] SiNWs functionalized with alkyl chains by the chlorination/alkylation process resisted oxidation with enhanced stability.[78–81]

Hydrosilylation is an important reaction to covalently bond organic molecules to hydrogen-terminated SiNWs, which can subsequently be used to immobilize biomaterials.[82,83] The hydrosilylated surface has fewer defects than the H-terminated surfaces or surfaces covered with native oxide.

SiNWs could be covalently modified with DNA oligonucleotides.[84] The covalent photochemical functionalization of hydrogen-terminated SiNWs grown on SiO_2 substrates enabled subsequent chemistry to form covalent adducts with DNA. This method provides a pathway for preparing functionalized SiNWs with well-defined chemical and biomolecular recognition properties. Subsequently, SiNWs were chemically bonded with single-stranded DNA or peptide nucleic acid probe molecules[85,86] (Figure 6).

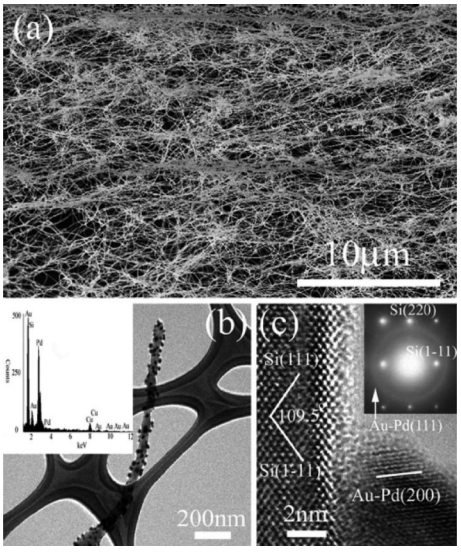

Figure 5. (a) SEM image of SiNWs, (b) TEM image of a single SiNW supported with Au–Pd nanoparticles and its EDX spectrum (inset) revealing an Au/Pd atomic ratio of 1.29:11.39, and (c) HRTEM image showing Si (111) and Au–Pd (200) crystal planes, and SAED pattern (inset) indicating bright Si diffraction spots and a weak Au–Pd diffraction ring.[72] Reprinted with permission from ref.[72]

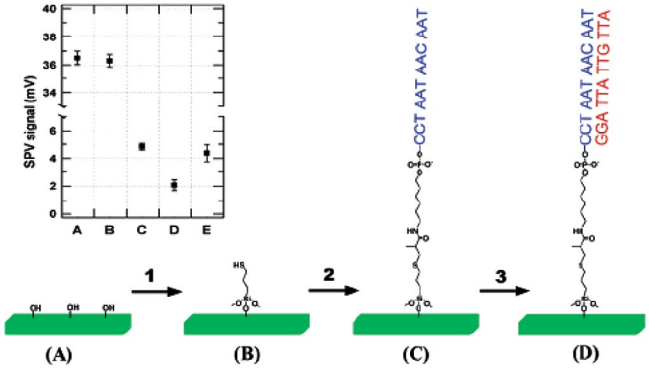

Figure 6. Modification scheme of the SiNW surface for the DNA detector: (1) self-assembly of 3-mercaptopropyltrimethoxysilane (MPTMS) by gas-phase reaction in Ar for 4 h; (2) covalent immobilization of DNA probes by exposing the previous surface to a 5 μM solution of oligonucleotide CCT AAT AAC AAT modified with acrylic phosphoramidite at the 5′-end for 12 h; (3) DNA detection based on hybridization between label-free complementary DNA target GGA TTA TTG TTA and the immobilized DNA probes on the SiNW surfaces. The inset is the surface photovoltage signal on a p-type Si surface at different stages of the modification; A, B, and C correspond to the schematic diagrams, D is with a 25 pM solution of complementary DNA target exposed to the surface C, and E is with 25 pM solution of noncomplementary DNA (GGA TCA TTG TTA) exposed to the surface C. Reprinted with permission from ref.[86]

2.3. Thermoelectricity and Giant Piezoresistance

The thermoelectric properties of SiNWs with different shapes, sizes, and orientations have been theoretically investigated by using the sp^3d^5s tight-binding model coupled with the ballistic transport approach. It was found that the thermoelectric properties are significantly dependent on nanowire geometry[87] (Figure 7).

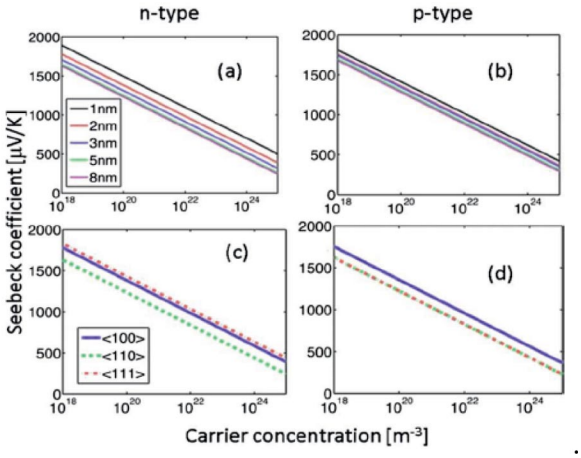

Figure 7. (a, b) Seebeck coefficient as a function of carrier concentration for n-type/p-type circle cross-section shape along the [100] orientation for silicon nanowires with various diameters of 1, 2, 3, 5, and 8 nm. (c and d) Dependence of orientation on Seebeck coefficient of circular nanowires with 2 nm diameter along the [100] (solid), [110] (dotted), and [111] (dashed) directions for n-type and p-types. Reprinted with permission from ref.[87]

Yang et al.[88] and Boukai et al.[89] reported that rough SiNWs of 200–300 nm diameter have Seebeck coefficients and electrical resistivity values that are the same as doped bulk Si, but those with diameters of about 50 nm exhibit a 100-fold reduction in thermal conductivity, yielding the thermoelectric figure of merit $ZT = 0.6$ at room temperature. For such SiNWs, the lattice contribution to thermal conductivity approaches the amorphous limit for Si, which cannot be explained by current theories. Bulk Si, however, has a high k (ca. 150 $W m^{-1} K^{-1}$ at room temperature),[88,90–92] giving $ZT < 0.01$ at 300 K. They reported that only chemically etched silicon showed interesting physical properties.

The main advantage of using SiNWs (p-type <100>-oriented, nominally 10–20 Ωcm) for thermoelectric applications lies in the large difference in the mean free path lengths of electrons and phonons at room temperature: 110 nm for electrons in highly doped samples and 300 nm for phonons.[92]

Another possibility to increase the figure of merit, ZT, is to functionalize the surface of SiNWs. Two examples of surface decorations were studied to illustrate the underlying ideas: nanotrees and alkyl-functionalized SiNWs. For both systems, Markussen et al. found that: (i) the phonon conductance is significantly reduced relative to the electronic conductance, leading to high ZT, and (ii) for ultrathin wires, surface decoration leads to significantly better performance than surface disorder.[93] Yang et al.[94] showed that SiNWs also exhibited giant piezoresistance effects.

Surface-dependent transport properties of SiNWs are important in their applications in field-effect transistors, electrochemistry, batteries, and solar cells. Chemical reactions and biomodification of SiNWs are important in catalyst, drug delivery, bioimaging, templating and sensing applications. Thermoelectricity and giant piezoresistance would find applications in energy recovery, micromachines, micro energy sources. Nevertheless, much work is needed to realize these potential applications.

3. Applications of SiNWs

Taking advantage of their surface-dependent physical and chemical properties, SiNWs may be developed for various applications in catalysis, devices, sensors, biosystems, batteries, and solar cells. Some of those applications are close to the market place.

3.1. Catalysis

It is well known that bulk Si has little or no catalytic activity. Remarkably, H-SiNWs were found to exhibit excellent photocatalytic activity in the degradation of rhodamine B.[71] H-SiNWs showed even better photocatalytic activities than Pd-, Au-, Rh-, or Ag-modified SiNWs, as shown in Figure 8.

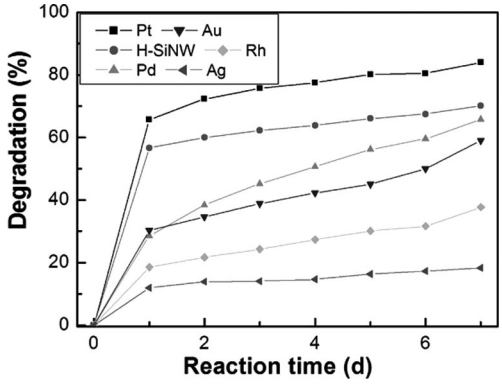

Figure 8. Degradation of rhodamine B vs. reaction times, under metal-modified SiNW catalysts, revealing that Pt-modified SiNWs have the best catalytic activity, followed by H-treated, Pd-modified, Au-modified, Rh-modified, and Ag-modified SiNWs. Reprinted with permission from ref.[71]

The catalytic activity may be attributed to the terminated hydrogen atom acting as an electron sink, which accelerates the separation of electron and hole, leading to increased photocatalytic efficiency. This discovery is important in the application of Si-related materials as they are normally employed as catalyst carriers or supports, taking advantage of their vast surface area, numerous and diameter-controlled voids, and acidic nature to balance the basicity of active metal components. Notably, catalysts based on SiNWs may be recycled and reused with little loss of catalytic ac-

tivity.[95–98] Noble metal nanoparticles supported and anchored on SiNWs are prevented from aggregation and growth in size, so that the catalysts would retain high efficiency during reaction and after recycling.

Au-Pd nanoparticles grown on the surface of SiNWs exhibited a mutual promotional effect in the degradation reaction of *p*-nitroaniline. These SiNW-supported Au–Pd catalysts provided higher catalytic activity than Pd/Si or Au/Si catalysts alone. The synergistic effect was calculated to have a factor of 2.35.[72] The excellent catalytic activity of Au-Pd/Si catalysts originated from the synergistic effect with Au, which acted as a promoter for the Pd/Si catalysts.

Tsang et al. reported that metal-modified (metal: Au, Cu) SiNWs are superior catalysts for selective oxidation of hydrocarbons,[99] and SiNWs are a powerful substrate support for nanocatalysts. AuNPs- and CuNPs-coated SiNWs catalysts can enable high selectivity and high efficiency in the oxidation of *cis*-cyclooctene to epoxycyclooctane (Figure 9). Significantly, oxidation by these catalysts using only air as oxidant with no solvent is truly "green chemistry".

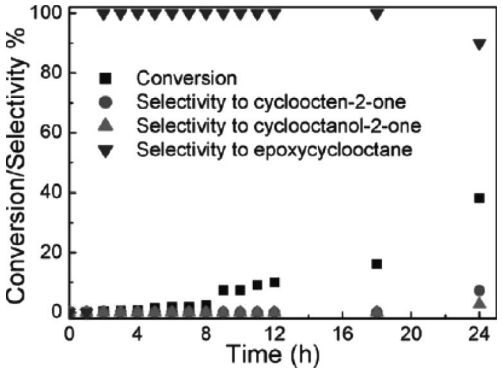

Figure 9. Reaction profile of oxidation catalyzed by Au/SiNWs. Reprinted with permission from ref.[99]

Chen et al. reported the degradation of environmentally hazardous dyes using SiNWs.[100] Environmentally unfriendly methyl red was degraded with the assistance of H-terminated SiNWs under ultrasonic agitation. After the degradation reaction, SiNWs can be regenerated by heating to desorb the organic species followed by subsequent treatment in hydrogen plasma to restore the hydrogen. It was reported that degradation of the organic dye is based on cleaving the N=N bonds through a reduction process by H-SiNWs with the assistance of ultrasonic agitation. The degradation rate of methyl red increases with the quantity of H-SiNWs or the ultrasonic agitation power.

SiNW showed remarkable photocatalytic activity, and SiNW-supported catalysts also revealed superior catalytic activity, high selectivity, and reproducibility. However, SiNW-based catalysts are not yet comparable to carbon-supported or bulk Si-supported catalysts with respect to catalytic activity, stability, and durability. More research on SiNW or SiNW-supported catalysts is needed.

3.2. Li Ion Batteries

SiNWs can improve the storage capacity for the lithium-ion-battery anode, since storage of a lithium ion generally needs six carbon atoms while four lithium ions can be stored in one silicon atom. Thus a Si electrode is anticipated to have a much higher storage capacity for Li than a carbon electrode.

Indeed, SiNW arrays were shown to be promising scalable anode materials for rechargeable lithium batteries.[101] In addition to being low-cost, large-area, and easy to prepare, the electroless-etched SiNWs have good conductivity, nanometer-scale rough surfaces, larger charge capacity, and longer cycling stability. These features facilitate charge transport and insertion/extraction of Li ions. The excellent performance of electroless-etched SiNWs for anode materials for lithium-ion batteries was demonstrated. Nevertheless, much work is needed to further improve SiNW-based anode batteries.

3.3. Templates

SiNWs can be employed as templates to prepare gold nanowires (AuNWs): when SiNWs coated with Au were furnace-annealed at approximately 880 °C at 10^{-2} Torr, uniform AuNWs were formed in the cores of SiNWs.[102] The formation of AuNWs is due to softening of the SiNWs upon oxidation and enhanced Au diffusion at elevated temperatures. The SiO_x shell of AuNWs can be removed by HF etching to expose the AuNWs.

Moreover, quasi-1D Ni nanostructures were synthesized by SiNW templating.[103] Ni ions were reduced to nanoparticles at 190 °C for approximately 1 h. Ni particles were assembled in a quasi-1D structure, which exhibited enhanced coercivity reaching 315.2 Oe at room temperature, much higher relative to 0.7 Oe for bulk Ni. SiNWs were also employed as templates to grow silica nanotubes,[104] and high-purity, single-crystalline beta-Si_3N_4 nanowires with diameters of 30 nm by a CVD process.[105]

3.4. Solar Cells

The key steps involved in solar cells are photon absorption, exciton transport, exciton dissociation/charge separation, and charge collection. From the material and device structure standpoint, high-aspect-ratio nanowires are promising candidates to convert photons to charges efficiently.[106–108] Therefore, a great deal of effort has been devoted to prepare various Si nanostructures for their potential applications in Si-based optoelectronic devices.

It has been shown that a solar cell based on SiNWs can achieve efficient absorption of sunlight by using only 1% of the active material required in a conventional solar cell.[109] The energy conversion efficiency of an optimal SiNW-based solar cell may reach 12%.[110]

3.4.1. Photon Absorption

The reduction of optical loss is an important consideration in obtaining high-efficiency Si solar cells. Peng et al. investigated the reflectance behavior of SiNW arrays and showed that, due to the ultrahigh surface area, the subwavelength-structured (SWS) surface, and the resemblance to a multi-antireflection coating, large-surface-area SiNW arrays exhibited remarkable antireflection ability.[111] Stelzner and co-workers also reported the significant reduction of reflectance and strong light trapping of nanowires.[112] Due to the high refractive index of a-Si:H, a large portion of incident light is reflected back from the surface of a-Si:H and a-Si:H nanostructures. The measured absorption of the nanowire arrays (85%) presents a significant advantage over the thin film counterpart (75%). Compared with flat thin films, nanowire arrays provided excellent impedance matching between a-Si: H and air through a gradual reduction of the effective refractive index away from the surface and therefore exhibited enhanced absorption due to large antireflection over a wide range of wavelengths and angles of incidence.[113] Also, the broadband optical absorption properties of SiNW films fabricated by wet etching and CVD are found to be higher than those of solid Si films of equivalent thickness, which is of interest in optoelectronic device applications.[114]

3.4.2. Charge Separation

Grossman and co-workers[115] presented a technique by morphology control at the nanoscale for the separation of charge carriers in SiNW solar cells that would eliminate the need for p-n doping, possibly allowing the use of substantially lower-quality Si without degrading the conversion efficiency, while concomitantly permitting simple, scalable changes in the manufacturing process. The technique may employ axial strain by breaking translational symmetry, such as functionalizing SiNWs with different chemical groups at their end surfaces, which attract each other and form longer chains to locate the HOMO and LUMO states separately in the building blocks with different functional groups. The results indicate that solar cells could be designed to separate charge carriers by morphology control in a nanomaterial, wherein thermalization of the photoexcited carriers would serve the beneficial purpose of driving electrons and holes to different spatial locations, as opposed to typical carrier diffusion in the p-n junctions of conventional solar cells.[115]

Another method to achieve efficient charge separation is by doping or blending with other materials. Peng et al. reported that coating of PtNPs on SiNW sidewalls yielded a substantial enhancement in a conformal radial charge-separating junction and an energy conversion efficiency of up to 8.14%[116] (Figure 10). Kalita et al. reported the fabrication of vertically aligned n-SiNW arrays and poly(3-octylthiophene) hybrid solar cells incorporating carbon nanotubes (CNTs).[117]

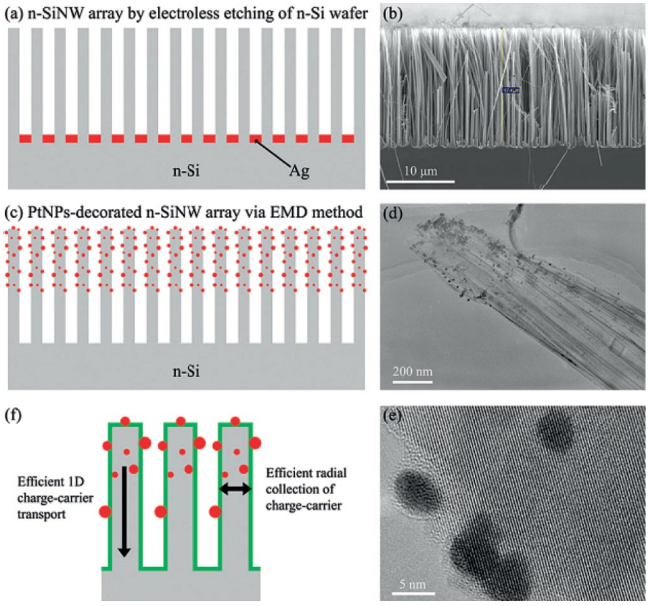

Figure 10. (a, c) Schematic of an n-SiNW array and a PtNP-decorated n-SiNW array prepared by chemical etching of a silicon wafer followed by electroless metal deposition. (b) Cross-sectional SEM image of as-prepared Si nanowire array; dendritic Ag can be observed inside the SiNW array. (d) Low-magnification TEM image of PtNP-decorated n-SiNWs showing PtNPs on the wire surface. (e) High-resolution TEM image of PtNP-decorated SiNW, revealing PtNP diameters of approximately 5 nm. (f) In addition to excellent light absorption and efficient radial charge-carrier collection, SiNWs have direct 1D electronic pathways allowing for efficient 1D charge-carrier transport along the length of every wire. The red dots denote PtNPs on n-SiNW surfaces and the green layer the space charge layer formed owing to the conformal contact between silicon and electrolyte. Reprinted with permission from ref.[116]

Lu and co-workers used the high-mobility inorganic quantum dots (QDs) and SiNWs as the charge transport channels to efficiently transfer electrons and holes, expecting to form a new solar cell paradigm.[118]

3.4.3. Charge Collection

Wang et al. reported that, since charge separation and collection only occur in the space-charge region, nanowires should not be significantly wider than the space-charge region. Maximum charge collection efficiency is therefore expected for moderately doped nanowires with optimum diameters of 200–300 nm and lengths of 10–30 mm.[119] Wang et al. used a double-wall nanotube film as the counterelectrode favorable for charge collection and transport with the redox electrolyte (HBr and Br_2). At a SiNW density of 0.150, this hybrid solar cell shows a conversion efficiency of 1.29%.[120] To improve contact and decrease resistance loss, Zhu et al. deposited continuous Ti/Pd/Ag electrode film on aligned SiNW arrays with a certain inclination, leading to improved current collection efficiency.[121] To mitigate the surface recombination issue, Gunawan et al. reported the application of a conformal Al_2O_3 film grown by atomic layer deposition to serve as an effective passivation layer,[122] yielding clear improvements of short-circuit current and open-circuit voltage.

SiNWs absorb light in the longitudinal (or axial) direction (>1 mm), and separate and collect charges in the transverse (or radial) direction (ca. 100 nm), thus easily circumventing the conflicting requirements described above. Lieber et al. reported p-type/intrinsic/n-type (p-i-n) coaxial SiNW solar cells, which integrated the key advantages of the core/shell architecture: that is, carrier separation takes place in the radial rather than the longer axial direction, and a radial carrier collection distance smaller than or comparable to the minority-carrier diffusion length.[107] The polycrystalline p-core could enhance light absorption and significantly reduce the recombination processes by improving the crystalline structure of the shells and/or passivating the surface and grain boundaries[123] of the nanowires.

The effects of several important parameters of nanowires, including length, diameter, and doping level, have been comprehensively studied and experimentally optimized to achieve high-efficiency solar cells. Initial efforts to study these parameters have been devoted primarily to individual nanowires[124] and a large number of nanowires in arrays ($>10^6$ mm^{-2}).

3.5. Biological Applications

Nanotechnology has received increased attention in biological research.[125,126] SiNWs have emerged as promising materials for biological applications such as tissue engineering, biosensors, and drug delivery.[127,128] SiNWs (d = 1–100 nm) are a few orders of magnitude smaller in diameter than mammalian cells (d_{cell} is approximately of the order of 10 μm) yet comparable to the sizes of various intracellular biomolecules. The nanowires have high aspect ratio ($< 10^3$) and yet are sufficiently rigid to sustain ready mechanical manipulation. The nanometer-scale diameter and the high aspect ratio of SiNWs make them readily accessible to the interiors of living cells, which may facilitate the study of the complex regulatory and signaling patterns at the molecular level.[129]

3.5.1. Cell Assay

For biomedical applications, compatibility in cellular assays is an important consideration. Fibroblasts are a prevalent cell line common to numerous connective tissue sites in vivo, and can serve as a useful starting point for all in vitro screening of the utility of these materials. Coffer et al. showed that the proliferation of fibroblast cells is not adversely affected by the presence of SiNWs.[130] They observed that the rate of growth of fibroblast cells in the presence of SiNWs is nearly the same as that of the growth of cells in the absence of nanowires.[130] These results indicated SiNWs are noncytotoxic towards fibroblast cells, and that they are promising and useful for future biomedical applications.

Yang et al.[131] reported a direct interface of SiNWs with mammalian cells, such as mouse embryonic stem (mES) cells and human embryonic kidney (HEK 293T) cells, without any external force. The cells were cultured on a Si substrate with a vertically aligned SiNW array (Figure 11). The penetration of the SiNW array into individual cells occurred naturally during cell incubation. The cells survived up to several days on the nanowire substrates, and their longevity was highly dependent on the diameter of SiNWs.

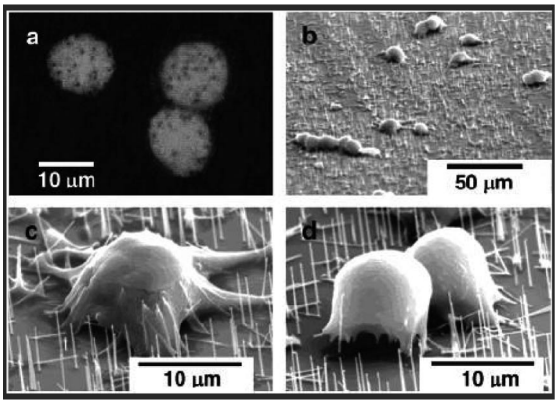

Figure 11. (a) A confocal microscopy image of mouse embryonic stem (mES) cells penetrated with SiNWs. (b) SEM image of mES cells on a nanowire array substrate. (c, d) SEM images of individual mES cells penetrated with SiNWs. Reprinted with permission from ref.[131]

3.5.2. Biorelevant Calcification

Interfacial effects can play a significant role in the biological activity of a biomaterial. The ability to tune the surface properties either by chemical or electrical variations at an implant surface adds useful functionality. There has been considerable interest in the field of tissue engineering to incorporate some sort of electroactive material in implants to modulate tissue regeneration by electrical bias. The ability to manipulate the surface of SiNWs by chemical modifications and electrical stimuli makes them interesting candidates for various biomedical applications. The extent of calcium phosphate formation on a biomaterial can be used as one criterion to evaluate its suitability for orthopedic applications. One convenient method to assess this bioactivity in vitro is to expose the material to a cellular simulated body fluid (SBF) that has ion concentrations nearly equal to those in human plasma.[132] Coffer et al.[130] presented a cathodic bias experiment performed in an electrochemical cell, in which the Si wafer with attached SiNWs was the working electrode, platinum foil the counterelectrode, and SBF solution the electrolyte. The results revealed the ability to control the extent of calcium phosphate formation on SiNWs through interfacial chemistry and associated electrochemical processes.

3.5.3. Gene Delivery

Yang et al.[131] reported preliminary results of gene delivery using a SiNW array. The HEK 293T cell line was cultured on SiNW substrates with DNA that was electrostatically deposited. Interestingly, the HEK cells did not adhere to flat silicon substrates under the same culturing conditions. This indicates that the penetration of SiNWs promotes the retention of cells on substrates and therefore gene

delivery. The low efficiency of transfection might be due to the difficulty of releasing the electrostatically bound DNA and can be improved with more sophisticated conjugation and release schemes.

3.5.4. Drug Delivery

The lack of proper control over a drug release rate and target delivery area is a serious disadvantage for conventional drug tablets. Biomaterials with nanoscale features have become increasingly popular as controlled release reservoirs for drug delivery.[133] Nanoscale drug delivery systems can be devised to tune the release kinetics, regulate biodistribution, adjust bioavailability over time, and minimize toxic side effects, thus enhancing the therapeutic index of a given drug. Biocompatible porous Si is an attractive material for controlled drug delivery applications for many reasons,[134–136] including the versatility and capability of tailoring the pore sizes (from micrometers to nanometers) and volume of the reservoir. There are numerous existing and convenient chemistries for surface modifications and surface reactions, by which SiNWs can be used as a template for designing polymeric nanostructures for unique optical properties and exceptional biosensing potential.[136]

Jin et al.[137] reported the drug release behavior of a different nanostructured porous Si template, namely, SiNW arrays with a high porosity and surface reactivity and a relatively large reservoir volume (Figure 12). They showed that SiNW carriers can maintain a drug release level and longevity for 42 days. The same study also reported the interesting behavior of SiNWs in preventing cell/protein adhesion.

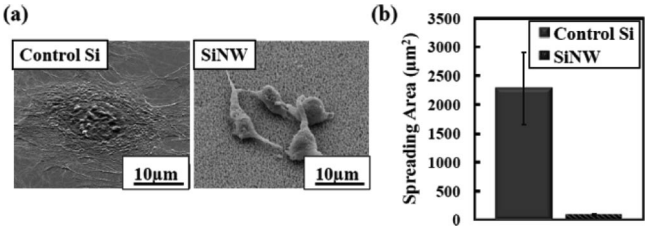

Figure 12. Cell spreading assay. (a) High-magnification SEM micrographs showing cell spreading on control Si and SiNW surfaces after 24 h of incubation. The cells on the SiNW surface are unable to spread and seemingly adhere to each other rather than to the surface. (b) Quantitative graph depicting the spreading area of cells by using the Image J software on the Si vs. SiNW surfaces. Cells simply do not spread on SiNW surfaces. Reprinted with permission from ref.[137]

3.5.5. Cell Adhesion and Spreading Behavior

Cell adhesion is the first step in the interaction of material with cells and is of fundamental importance in the development and maintenance of tissues. Yang et al.[138] have studied the interactions between biological cells and SiNW arrays and how SiNW arrays affect cellular behavior such as cell adhesion and spreading. They observed that no cell was attached to the side of a SiNW or to the bottom of the wire array. The spreading profile of the cells on the SiNW array was different from that on the flat Si wafer. The cells on the SiNW array did not stretch out as freely as those on a flat Si wafer, therefore resulting in relatively smaller cell sizes. The viability of cells incubated on the SiNW array was evaluated by using an Alamar Blue assay. The results indicated that the SiNW array showed biocompatibility similar to that of other nanowire structures. The SiNW arrays influenced cell adhesion and spreading in two aspects: enhancing the cell–substrate focal adhesion force and restricting cell spreading.

3.5.6. In Vivo and In Vitro Imaging of SiNWs

SiNWs have unparalleled dimension-control properties with variation in diameters ranging from 3 to 100 nm and lengths from a few hundred nanometers to tens of micrometers. Yang et al.[139] reported strong and stable third-order nonlinear optical (NLO) signals, including four-wave mixing (FWM) and third-harmonic generation (THG), from SiNWs of diameters as small as 5 nm. They further employed such signals to monitor SiNWs circulating in the peripheral blood of a live mouse and to map the organ distribution of systematically administered SiNWs.

These properties suggest exciting opportunities for the use of SiNWs as a novel in vivo imaging agent offering intrinsic 3D spatial resolution, high photostability, and orientational information. With the advantages of highly controllable dimensions, versatile surface chemistry, and intensive intrinsic NLO signals, SiNWs provide a promising nanobiological system for investigating cellular interactions with 1D nanomaterials.

3.6. Sensors

SiNWs may serve as excellent candidates for sensors, partly because they are environmentally friendly, biologically compatible, easy to prepare, and convenient to modify. SiNW-based sensors are mostly based on the transistor principle, especially field-effect transistors. SiNW-based sensors based on other working principles have also been fabricated. Noble metals (silver or gold) were readily reduced and coated on the surface of H-terminated SiNWs, which can serve as substrates in surface-enhanced Raman scattering (SERS) or fluorescence detection. High SERS sensitivities are obtained as a result of the strong surface plasmon resonance between the noble metal nanoparticles. Electrochemical sensors based on SiNWs were also reported to have wide linearity, good repeatability, and long shelf life.

3.6.1. Surface-Enhanced Raman Scattering (SERS) and Surface-Enhanced Fluorescence

SiNWs coated with metal nanoparticles, such as Ag, Cu, Pd, Co, Au, and Pt, were employed as substrates for SERS analysis. An extremely strong Raman signal was observed with a detection limit of about 600 molecules.[140]

SiNWs modified with gold nanoparticles were used to improve electrochemical sensors based on acetyl cholinesterase for pesticide detection, enabling the detection of di-

chlorvos at a low concentration of 8 ng/L.[141] Gold nanoparticles were deposited by chemical vapor deposition on SiNWs, and they were capable of enhancing Raman signals based on SERS effect. In the same experiment, gold may be replaced with silver to yield Raman signals that are even more enhanced.[142]

Substrates based on SiNWs coated with Ag nanoparticles and used to detect rhodamine 6G, crystal violet, nicotine, and calf thymus DNA (CT DNA) yielded ultrahigh SERS sensitivity[143] (Figure 13). Moreover, they exhibited great potential for ultrasensitive molecular sensing in SERS detection of *Bacillus anthracis* spores, achieving a limit of detection of approximately 4×10^{-6} M calcium dipicolinate, a biomarker for anthrax.[144] They were used as substrates for SERS and hyper-Raman spectroscopy to examine Rhodamine 6G, crystal violet, a cyanine dye, and a cationic donor/acceptor-substituted stilbene.[145] Furthermore, SiNWs were coated with silver nanoparticles by in situ electroless metal deposition.[146] They showed large Raman scattering enhancement for rhodamine 6G with a detection limit of 10^{-14} M.

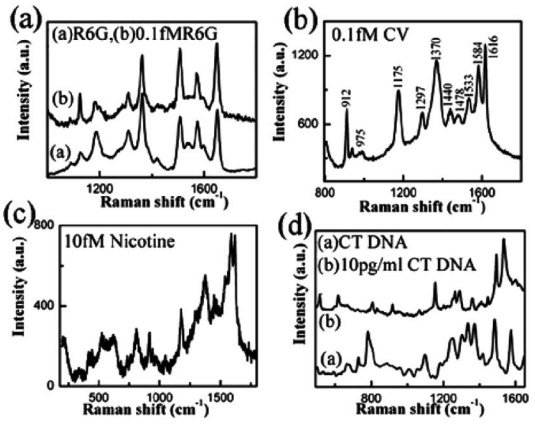

Figure 13. Raman spectra obtained from Ag-modified SiNWs coated with 25 μL of (a) 1×10^{-16} M R6G solution, (b) 1×10^{-16} M crystal violet solution, (c) 1×10^{-14} M nicotine solution, and (d) 1×10^{-8} mg/mL CT DNA solution in water. Curves (a) in (a) and (d) are the Raman spectra collected from R6G powder and solid CT DNA, respectively. Reprinted with permission from ref.[143]

Zhang et al. reported the fabrication of SERS substrates based on SiNW arrays by etching Si wafer to form uniform SiNWs followed by coating with Ag nanoparticles by electroless deposition. Such SERS substrates can enable the detection of trace amounts of immunoglobulin and monitor immunoreactions.[147] The 3D arrangement of Ag nanoparticles@SiNW arrays offered significant advantages over long interaction distances. The same substrate offered a SERS enhancement factor of 8–10 orders in the detection of Sudan dye molecules.[148] The substrate was also used to quantitatively detect the pesticide carbaryl at concentrations down to 10^{-7} M.[149]

A microchannel composed of a SiNW array and Ag nanoparticles was fabricated on a Si wafer by using wet etching, and it served to improve the detection sensitivity of bovine serum albumin by SERS with a concentration as low as 1 pM.[150] Gold droplets on SiNWs can act as efficient probes for SERS and tip-enhanced Raman spectroscopy to detect malachite green,[151] DNA, and bacteria.[152]

SiNWs coated with Ag nanoparticles show excellent surface-enhanced fluorescence of lanthanide ions, such as Pr^{3+}, Nd^{3+}, Ho^{3+}, and Er^{3+}, with a markedly enhanced factor of hundreds of times (Figure 14). These results may be explained by the local field overlap arising from the closed and fixed silver nanoparticles on SiNWs.[153]

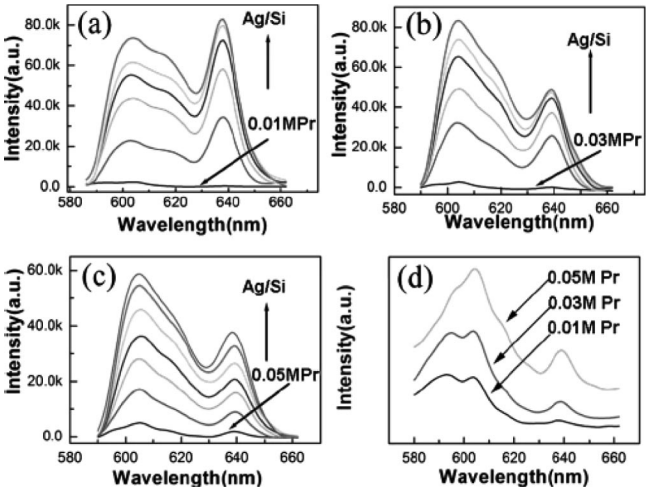

Figure 14. Fluorescence spectra at different Pr^{3+} concentrations with the addition of Ag/Si nanomaterials. Concentration of Pr^{3+} (a) 0.01 M, (b) 0.03 M, (c) 0.05 M; and (d) fluorescence spectra at different concentrations of Pr^{3+} without Ag/Si nanomaterials. Reprinted with permission from ref.[153]

3.6.2. Electrochemistry

SiNWs were modified with gold nanoparticles and employed to fabricate working electrodes for the detection of bovine serum albumin[154] and glutathione by cyclic voltammetry,[155] which showed high sensitivity, wide linear concentration range, and fast response (Figure 15).

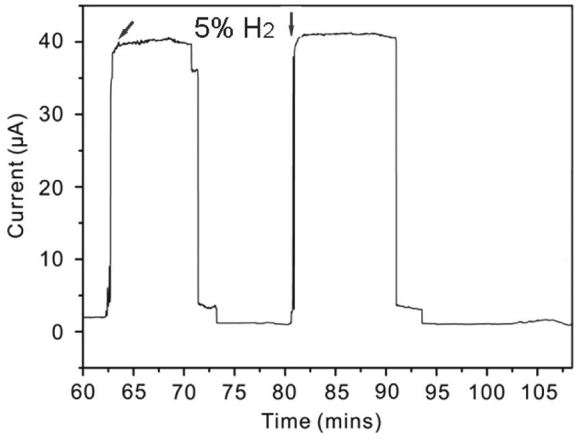

Figure 15. Real-time current response of Pd-coated SiNWs in 5% H_2. Reprinted with permission from ref.[160]

Wan et al. used Pd-Ni co-deposited SiNWs as the working electrode to detect ethanol by cyclic voltammetry and fixed potential amperometry techniques with a sensitivity of 0.76 mA mM^{-1} cm^{-2} and a detection limit of 10 μM.[156]

SiNWs were used as pH sensors[34,157] and for glucose detection.[158] SiNWs modified with boron and magnesium were employed as sensors to detect glucose and hydrogen peroxide, respectively. These sensors exhibited a wide linear concentration detection range, high sensitivity, good reproducibility, and long-term stability.[159] Pd-modified SiNWs were used as H_2 gas sensors,[160] which showed high sensitivity and fast response (Figure 15). SiNWs, upon exposure to ammonia gas and water vapor, were found to dramatically decrease in electrical resistance at room temperature. The detection showed fast response, high sensitivity, and reversibility.[161]

3.6.3. Field-Effect Transistors (FET)

Among biosensors of various types, SiNW field-effect transistors are among the most sensitive and powerful devices for biological applications.

A single SiNW was modified with 3-mercaptopropyltriethoxysilane and fabricated as a field-effect transistor, which showed high sensitivity in the detection of heavy metal ions Hg^{2+} and Cd^{2+} at concentrations down to 10^{-7} and 10^{-4} M, respectively.[162] A SiNW field-effect transistor was used to detect deoxyribonucleic acid with a detection limit in the sub-femtomolar level. Mismatched DNA sequences, including one- and five-base-mismatched DNA strands, could be distinguished from a complementary DNA gene by this label-free nanowire FET sensor.[163]

Fluorescent SiNWs were covalently modified with a fluorescent ligand, *N*-(quinoline-8-yl)-2-(3-triethoxysilylpropylamino)acetamide, and employed to detect Cu^{2+} at a low concentration of 10^{-8} M (Figure 16). This fluorescence sensor exhibited excellent sensitivity, selectivity, and reversibility.[164]

The functionalized polycrystalline SiNW field-effect transistor was demonstrated to achieve specific and ultrasensitive (at fM level) detection of the highly pathogenic strain (H5 and H7) virus DNA of avian influenza. This FET was modified with a complementary captured DNA probe and target DNA (H5) in the fM to pM range.[165] Specific electric changes were observed for streptavidin and avidin sensing in the sub-pM to nM range.[166]

The SiNW FET, placed in a microfluidic channel, exhibited change in linear conductance with changes in the ionic strength and composition of the electrolyte solution.[167] Delta (5)-3-ketosteroid isomerase was chemically modified with SiNW and served as a steroid acceptor with ensitivity at femtomolar level.[168]

SiNWs were covalently modified with crown ethers terminated with amine groups to recognize Na^+ and K^+, achieving an ultralow detection limit down to 50 nM.[83] They were also modified with a biologically relevant amino acid, phosphotyrosine, and fabricated into a FET to detect calcium up to 10 μM.[169]

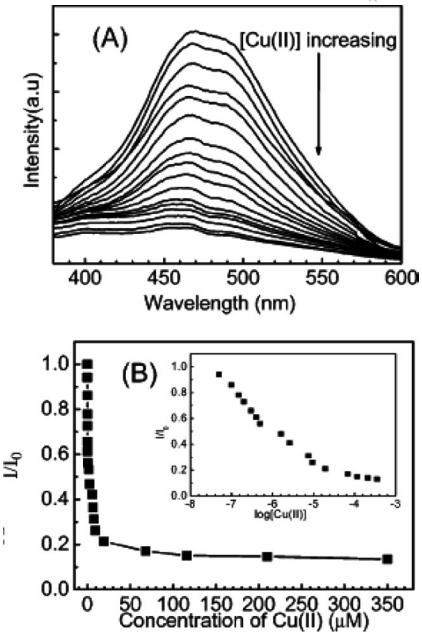

Figure 16. Fluorescence spectra (A) and titration curve (B) of QlOEt-modified SiNWs (68 μg/mL: 9×10^{-6} M QlOEt) with Cu^{II}. EtOH/water solution (30%) of 0.05 M HEPES buffer (pH 7.0). λ_{ex} = 324 nm, λ_{em} = 490 nm. Reprinted with permission from ref.[164]

A SiNW-based FET was biofunctionalized with peptide nucleic acid by using 3-maleimidopropionic acid *N*-hydroxysuccinimide ester and it was employed successfully for label-free DNA/PNA hybridization detection.[170] SiNW FET was used to detect target DNA.[128,171]

3.6.4. Logic Gates

A SiNW-based three-input (pH Hg^{2+} and Cl^-), chemically controlled logic gate, which combines the YES and INH operations, was realized by surface modification of SiNWs (Figure 17). A schematic representation of the logic

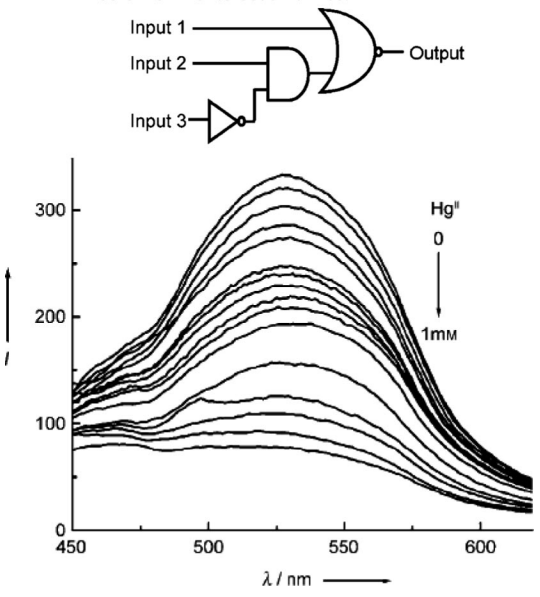

Figure 17. Fluorescence spectra of 1 (48 mg mL^{-1}) with increasing concentration of Hg^{II} ions in aqueous solution containing 4% CH_3CN (λ_{ex} = 330 nm). Reprinted with permission from ref.[172]

gates combining the YES and INH operations is given in the upper part of Figure 17. The fluorescence intensity was monitored as the output.[172]

4. Conclusions

SiNWs hold high promise for wide-ranging applications, partly due to their compatibility with conventional Si microtechnology. Furthermore, they show unique and unparalleled catalytic, optical, sensing, thermoelectrics, and piezoresistance properties. To achieve the full application potential of SiNWs, control and manipulation of their properties, size, and shape are essential. While great progress has been made in recent years, many challenges remain, and further research efforts are warranted.

Acknowledgments

The project was supported by the Research Grants Council of Hong Kong SAR (CityU5/CRF/08 and CityU101909) and the National Basic Research Program of China (973 Program) (Grant Nos. 2006CB933000 and 2010CB934502).

[1] A. M. Morales, C. M. Lieber, *Science* **1998**, *279*, 208–211.
[2] Y. F. Zhang, Y. H. Tang, N. Wang, D. P. Yu, C. S. Lee, I. Bello, S. T. Lee, *Appl. Phys. Lett.* **1998**, *72*, 1835–1837.
[3] T. E. Bogart, S. Dey, K.-K. Lew, S. E. Mohney, J. M. Redwing, *Adv. Mater.* **2005**, *17*, 114–117.
[4] R. S. Wagner, W. C. Ellis, *Appl. Phys. Lett.* **1964**, *4*, 89–90.
[5] Y. Cui, L. J. Lauhon, M. S. Gudiksen, J. Wang, C. M. Lieber, *Appl. Phys. Lett.* **2001**, *78*, 2214–2216.
[6] R. S. Wagner, W. C. Ellis, K. A. Jackson, S. M. Arnold, *J. Appl. Phys.* **1964**, *35*, 2993–3000.
[7] J. Westwater, D. P. Gosain, S. Usui, *Jpn. J. Appl. Phys. Part 1* **1997**, *36*, 6204–6209.
[8] A. I. Hochbaum, R. Fan, R. R. He, P. D. Yang, *Nano Lett.* **2005**, *5*, 457–460.
[9] S. Hofmann, C. Ducati, R. J. Neill, S. Piscanec, A. C. Ferrari, J. Geng, R. E. Dunin-Borkowski, J. Robertson, *J. Appl. Phys.* **2003**, *94*, 6005–6012.
[10] S. Sharma, M. K. Sunkara, *Nanotechnology* **2004**, *15*, 130–134.
[11] F. Iacopi, P. M. Vereecken, M. Schaekers, M. Caymax, N. Moelans, B. Blanpain, O. Richard, C. Detavernier, H. Griffiths, *Nanotechnology* **2007**, *18*, 505307.
[12] P. J. Alet, L. Yu, G. Patriarche, S. Palacin, P. Roca i Cabarrocas, *J. Mater. Chem.* **2008**, *18*, 5187–5189.
[13] C. Y. Wen, M. C. Reuter, J. Tersoff, E. A. Stach, F. M. Ross, *Nano Lett.* **2010**, *10*, 514–519.
[14] L. W. Yu, B. O'Donnell, P. J. Alet, S. Conesa-Boj, F. Peiro, J. Arbiol, P. I. R. Cabarrocas, *Nanotechnology* **2009**, *20*, 225604.
[15] I. Zardo, L. Yu, S. Conesa-Boj, S. Estrade, P. J. Alet, J. Roessler, M. Frimmer, P. R. I. Cabarrocas, F. Peiro, J. Arbiol, J. R. Morante, A. F. I. Morral, *Nanotechnology* **2009**, *20*, 155602.
[16] Y. W. Wang, J. Bauer, S. Senz, O. Breitenstein, U. Gosele, *Appl. Phys. A* **2010**, *99*, 705–709.
[17] Y. Wu, R. Fan, P. D. Yang, *Nano Lett.* **2002**, *2*, 83–86.
[18] M. W. Shao, L. Cheng, M. L. Zhang, D. D. D. Ma, J. A. Zapien, S. T. Lee, X. H. Zhang, *Appl. Phys. Lett.* **2009**, *95*, 143110.
[19] X. H. Fan, L. Xu, C. P. Li, Y. F. Zheng, C. S. Lee, S. T. Lee, *Chem. Phys. Lett.* **2001**, *334*, 229–232.
[20] Z. Zhang, X. H. Fan, L. Xu, C. S. Lee, S. T. Lee, *Chem. Phys. Lett.* **2001**, *337*, 18–24.
[21] S. T. Lee, Y. F. Zhang, N. Wang, Y. H. Tang, I. Bello, C. S. Lee, *J. Mater. Res.* **1999**, *14*, 4503–4507.
[22] C. P. Li, N. Wang, S. P. Wong, C. S. Lee, S. T. Lee, *Adv. Mater.* **2002**, *14*, 218–221.
[23] Y. Yao, F. H. Li, S. T. Lee, *Chem. Phys. Lett.* **2005**, *406*, 381–385.
[24] X. Duan, C. M. Lieber, *Adv. Mater.* **2000**, *12*, 298–302.
[25] D. P. Yu, Z. G. Bai, Y. Ding, Q. L. Hang, H. Z. Zhang, J. J. Wang, Y. H. Zou, W. Qian, G. C. Xiong, H. T. Zhou, S. Q. Feng, *Appl. Phys. Lett.* **1998**, *72*, 3458–3460.
[26] N. Wang, Y. H. Tang, Y. F. Zhang, D. P. Yu, C. S. Lee, I. Bello, S. T. Lee, *Chem. Phys. Lett.* **1998**, *283*, 368–372.
[27] W. S. Shi, H. Y. Peng, Y. F. Zheng, N. Wang, N. G. Shang, Z. W. Pan, C. S. Lee, S. T. Lee, *Adv. Mater.* **2000**, *12*, 1343–1345.
[28] Y. H. Tang, Y. F. Zhang, N. Wang, C. S. Lee, X. D. Han, I. Bello, S. T. Lee, *J. Appl. Phys.* **1999**, *85*, 7981–7983.
[29] C. P. Li, X. H. Sun, N. B. Wong, C. S. Lee, S. T. Lee, B. K. Teo, *Chem. Phys. Lett.* **2002**, *365*, 22–26.
[30] B. K. Teo, C. P. Li, X. H. Sun, N. B. Wong, S. T. Lee, *Inorg. Chem.* **2003**, *42*, 6723–6728.
[31] H. Y. Peng, Z. W. Pan, L. Xu, X. H. Fan, N. Wang, C. S. Lee, S. T. Lee, *Adv. Mater.* **2001**, *13*, 317–320.
[32] M. W. Shao, Y. Fu, L. Cheng, X. H. Wang, D. D. D. Ma, S. T. Lee, *J. Mater. Sci.: Mater. Electron.* **2009**, *20*, 1200–1202.
[33] F. M. Kolb, H. Hofmeister, R. Scholz, M. Zacharias, U. Gosele, D. D. D. Ma, S. T. Lee, *J. Electrochem. Soc.* **2004**, *151*, G472–G475.
[34] N. Wang, Y. F. Zhang, Y. H. Tang, C. S. Lee, S. T. Lee, *Appl. Phys. Lett.* **1998**, *73*, 3902–3904.
[35] Y. F. Zhang, Y. H. Tang, N. Wang, D. P. Yu, C. S. Lee, I. Bello, S. T. Lee, *Appl. Phys. Lett.* **1998**, *72*, 1835–1837.
[36] Y. F. Zhang, Y. H. Tang, H. Y. Peng, N. Wang, C. S. Lee, I. Bello, S. T. Lee, *Appl. Phys. Lett.* **1999**, *75*, 1842–1844.
[37] M. L. Zhang, K. Q. Peng, X. Fan, J. S. Jie, R. Q. Zhang, *J. Phys. Chem. C* **2008**, *112*, 4444–4450.
[38] K. Q. Peng, J. J. Hu, Y. J. Yan, Y. Wu, H. Fang, Y. Xu, S. T. Lee, J. Zhu, *Adv. Funct. Mater.* **2006**, *16*, 387–394.
[39] K. Q. Peng, Y. J. Yan, S. P. Gao, J. Zhu, *Adv. Funct. Mater.* **2003**, *13*, 127–132.
[40] K. Q. Peng, Y. Wu, H. Fang, X. Y. Zhong, Y. Xu, J. Zhu, *Angew. Chem. Int. Ed.* **2005**, *44*, 2737–2742.
[41] V. A. Sivakov, G. Bronstrup, B. Pecz, A. Berger, G. Z. Radnoczi, M. Krause, S. H. Christiansen, *J. Phys. Chem. C* **2010**, *114*, 3798–3803.
[42] K. Q. Peng, M. L. Zhang, A. J. Lu, N. B. Wong, R. Q. Zhang, S. T. Lee, *Appl. Phys. Lett.* **2007**, *90*, 163123.
[43] Z. Huang, H. Fang, J. Zhu, *Adv. Mater.* **2007**, *19*, 744–748.
[44] K. Q. Peng, A. J. Lu, R. Q. Zhang, S. T. Lee, *Adv. Funct. Mater.* **2008**, *18*, 3026–3035.
[45] J. D. Holmes, K. P. Johnston, R. C. Doty, B. A. Korgel, *Science* **2000**, *287*, 1471–1473.
[46] X. M. Lu, T. Hanrath, K. P. Johnston, B. A. Korgel, *Nano Lett.* **2003**, *3*, 93–99.
[47] H. Y. Tuan, A. Ghezelbash, B. A. Korgel, *Chem. Mater.* **2008**, *20*, 2306–2313.
[48] H. Y. Tuan, D. C. Lee, T. Hanrath, B. A. Korgel, *Nano Lett.* **2005**, *5*, 681–684.
[49] A. T. Heitsch, D. D. Fanfair, H. Y. Tuan, B. A. Korgel, *J. Am. Chem. Soc.* **2008**, *130*, 5436–5437.
[50] J. Bauer, F. Fleischer, O. Breitenstein, L. Schubert, P. Werner, U. Gosele, M. Zacharias, *Appl. Phys. Lett.* **2007**, *90*, 012105.
[51] B. Fuhrmann, H. S. Leipner, H. Hoche, L. Schubert, P. Werner, U. Gosele, *Nano Lett.* **2005**, *5*, 2524–2527.
[52] P. Werner, N. D. Zakharov, G. Gerth, L. Schubert, U. Gosele, *Int. J. Mater. Res.* **2006**, *97*, 1008–1015.
[53] P. D. Kanungo, N. Zakharov, J. Bauer, O. Breitenstein, P. Werner, U. Goesele, *Appl. Phys. Lett.* **2008**, *92*, 263107.
[54] N. D. Zakharov, P. Werner, G. Gerth, L. Schubert, L. Sokolov, U. Gosele, *J. Cryst. Growth* **2006**, *290*, 6–10.

[55] L. Schubert, P. Werner, N. D. Zakharov, G. Gerth, F. M. Kolb, L. Long, U. Gosele, T. Y. Tan, *Appl. Phys. Lett.* **2004**, *84*, 4968.
[56] V. Sivakov, G. Andra, U. Gosele, S. Christiansen, *Phys. Status Solidi A* **2006**, *203*, 3692–3698.
[57] V. G. Dubrovski, I. P. Soshnikov, N. V. Sibirev, G. E. Cirlin, V. M. Ustinov, M. Tchernycheva, J. C. Harmand, *Semiconductors* **2007**, *41*, 865–874.
[58] M. W. Shao, H. Hu, M. Li, H. Z. Ban, M. Y. Wang, J. Jiang, *Chem. Commun.* **2007**, 793–794.
[59] H. Nagayoshi, H. Nordmark, R. Holmestad, N. Matsumoto, S. Nishimura, K. Terashima, J. C. Walmsley, A. Ulyashin, *Jpn. J. Appl. Phys.* **2008**, *47*, 4807–4809.
[60] Y. H. Tang, L. Z. Pei, L. W. Lin, X. X. Li, *J. Appl. Phys.* **2009**, *105*, 044301.
[61] L. Z. Pei, Y. H. Tang, Y. W. Chen, C. Guo, W. Zhang, Y. Zhang, *J. Cryst. Growth* **2006**, *289*, 423–427.
[62] O. Englander, D. Christensen, J. Kim, L. Lin, S. J. S. Morris, *Nano Lett.* **2005**, *5*, 705–708.
[63] J. S. Jie, W. J. Zhang, K. Q. Peng, G. D. Yuan, C. S. Lee, S. T. Lee, *Adv. Func. Mater.* **2008**, *18*, 3251–3257.
[64] G. D. Yuan, Y. B. Zhou, C. S. Guo, W. J. Zhang, Y. B. Tang, Y. Q. Li, Z. H. Chen, Z. B. He, X. J. Zhang, P. F. Wang, I. Bello, R. Q. Zhang, C. S. Lee, S. T. Lee, *ACS Nano* **2010**, *4*, 3045–3052.
[65] C. S. Guo, L. B. Luo, G. D. Yuan, X. B. Yang, R. Q. Zhang, W. J. Zhang, S. T. Lee, *Angew. Chem. Int. Ed.* **2009**, *48*, 9896–9900.
[66] S. X. Zhang, E. R. Hemesath, D. E. Perea, E. Wijaya, J. L. Lensch-Falk, L. J. Lauhon, *Nano Lett.* **2009**, *9*, 3268–3274.
[67] X. H. Sun, C. P. Li, N. B. Wong, C. S. Lee, S. T. Lee, B. K. Teo, *J. Am. Chem. Soc.* **2002**, *124*, 14856–14857.
[68] C. P. Li, B. K. Teo, X. H. Sun, N. B. Wong, S. T. Lee, *Chem. Mater.* **2005**, *17*, 5780–5788.
[69] X. H. Sun, S. D. Wang, N. B. Wong, D. D. D. Ma, S. T. Lee, B. K. Teo, *Inorg. Chem.* **2003**, *42*, 2398–2404.
[70] X. H. Sun, C. P. Li, N. B. Wong, C. S. Lee, S. T. Lee, *Inorg. Chem.* **2002**, *41*, 4331–4336.
[71] M. W. Shao, L. Cheng, X. H. Zhang, D. D. D. Ma, S. T. Lee, *J. Am. Chem. Soc.* **2009**, *131*, 17738–17739.
[72] M. W. Shao, H. Wang, M. L. Zhang, D. D. D. Ma, S. T. Lee, *Appl. Phys. Lett.* **2008**, *93*, 243110.
[73] M. W. Shao, H. Wang, Y. Fu, J. Hua, D. D. D. Ma, *J. Chem. Sci.* **2009**, *121*, 323–327.
[74] X. H. Sun, N. B. Wong, C. P. Li, S. T. Lee, P. S. G. Kim, T. K. Sham, *Chem. Mater.* **2004**, *16*, 1143–1152.
[75] X. H. Sun, R. Sammynaiken, S. J. Naftel, Y. H. Tang, P. Zhang, P. S. Kim, T. K. Sham, X. H. Fan, Y. F. Zhang, C. S. Lee, S. T. Lee, N. B. Wong, Y. F. Hu, K. H. Tan, *Chem. Mater.* **2002**, *14*, 2519–2526.
[76] M. Nolan, S. O'Callaghan, G. Fagas, J. C. Greer, T. Frauenheim, *Nano Lett.* **2007**, *7*, 34–38.
[77] R. Haight, L. Sekaric, A. Afzali, D. Newns, *Nano Lett.* **2009**, *9*, 3165–3170.
[78] M. Y. Bashouti, T. Stelzner, S. Christiansen, H. Haick, *J. Phys. Chem. C* **2009**, *113*, 14823–14828.
[79] M. Y. Bashouti, Y. Paska, S. R. Puniredd, T. Stelzner, S. Christiansen, H. Haick, *Phys. Chem. Chem. Phys.* **2009**, *11*, 3845–3848.
[80] M. Y. Bashouti, T. Stelzner, A. Berger, S. Christiansen, H. Haick, *J. Phys. Chem. C* **2008**, *112*, 19168–19172.
[81] H. Haick, P. T. Hurley, A. I. Hochbaum, P. D. Yang, N. S. Lewis, *J. Am. Chem. Soc.* **2006**, *128*, 8990–8991.
[82] G. J. Zhang, J. H. Chua, R. E. Chee, A. Agarwal, S. M. Wong, K. D. Buddharaju, N. Balasubramanian, *Biosens. Bioelectron.* **2008**, *23*, 1701–1707.
[83] G. J. Zhang, A. Agarwal, K. D. Buddharaju, N. Singh, Z. Q. Gao, *Appl. Phys. Lett.* **2007**, *90*, 233903.
[84] J. A. Streifer, H. Kim, B. M. Nichols, R. J. Hamers, *Nanotechnology* **2005**, *16*, 1868–1873.
[85] Z. Li, B. Rajendran, T. I. Kamins, X. Li, Y. Chen, R. S. Williams, *Appl. Phys. A* **2005**, *80*, 1257–1263.
[86] Z. Li, Y. Chen, X. Li, T. I. Kamins, K. Nauka, R. S. Williams, *Nano Lett.* **2004**, *4*, 245–247.
[87] G. C. Liang, W. Huang, C. S. Koong, J. S. Wang, J. H. Lan, *J. Appl. Phys.* **2010**, *107*, 014317.
[88] A. I. Hochbaum, R. Chen, R. D. Delgado, W. Liang, E. C. Garnett, M. Najarian, A. Majumdar, P. D. Yang, *Nature* **2008**, *451*, 163–165.
[89] A. I. Boukai, Y. Bunimovich, J. Tahir-Kheli, J. K. Yu, W. A. Goddard, J. R. Heath, *Nature* **2008**, *451*, 168–171.
[90] M. Asheghi, Y. K. Leung, S. S. Wong, K. E. Goodson, *Appl. Phys. Lett.* **1997**, *71*, 1798–1800.
[91] M. Asheghi, M. N. Touzelbaev, K. E. Goodson, Y. K. Leung, S. S. Wong, *Heat Transf.* **1998**, *120*, 30–36.
[92] Y. S. Ju, K. E. Goodson, *Appl. Phys. Lett.* **1999**, *74*, 3005–3007.
[93] T. Markussen, A. P. Jauho, M. Brandbyge, *Phys. Rev. Lett.* **2009**, *103*, 055502.
[94] R. R. He, P. D. Yang, *Nature Nanotechnol.* **2006**, *1*, 42–46.
[95] H. Hu, M. W. Shao, W. Zhang, L. Lu, H. Wang, S. Wang, *J. Phys. Chem. C* **2007**, *111*, 3467–3470.
[96] F. X. Wang, M. W. Shao, L. Cheng, D. Y. Chen, Y. Fu, D. D. D. Ma, *Mater. Resear. Bull.* **2009**, *44*, 126–129.
[97] J. Hua, M. W. Shao, L. Cheng, Y. Fu, D. D. D. Ma, *J. Phys. Chem. Solids* **2009**, *70*, 192–196.
[98] H. T. Yu, X. Y. Li, X. Quan, S. Chen, Y. B. Zhang, *Enviro. Sci. Tech.* **2009**, *43*, 7849–7855.
[99] C. H. A. Tsang, Y. Liu, Z. H. Kang, D. D. D. Ma, N. B. Wong, S. T. Lee, *Chem. Commun.* **2009**, *39*, 5829–5831.
[100] Z. H. Chen, Y. B. Tang, Y. Liu, Z. H. Kang, X. J. Zhang, X. Fan, C. S. Lee, I. Bello, W. J. Zhang, S. T. Lee, *J. Appl. Phys.* **2009**, *105*, 034307.
[101] K. Q. Peng, J. S. Jie, W. J. Zhang, S. T. Lee, *Appl. Phys. Lett.* **2008**, *93*, 033105.
[102] T. C. Wong, C. P. Li, R. Q. Zhang, S. T. Lee, *Appl. Phys. Lett.* **2004**, *84*, 407–409.
[103] M. W. Shao, G. X. Qian, H. Z. Ban, M. Li, H. Hu, L. Lu, P. Zhang, *Scripta Mater.* **2006**, *55*, 851–854.
[104] R. Fan, Y. Y. Wu, D. Y. Li, M. Yue, A. Majumdar, P. D. Yang, *J. Am. Chem. Soc.* **2003**, *125*, 5254–5255.
[105] J. J. Niu, J. N. Wang, *Chem. Vapor Depos.* **2007**, *13*, 396–400.
[106] J. R. Maiolo, B. M. Kayes, M. A. Filler, M. C. Putnam, M. D. Kelzenberg, H. A. Atwater, N. S. Lewis, *J. Am. Chem. Soc.* **2007**, *129*, 12346–12347.
[107] B. M. Kayes, H. A. Atwater, N. S. Lewis, *J. Appl. Phys.* **2005**, *97*, 114302.
[108] A. P. Goodey, S. M. Eichfeld, K. K. Lew, J. M. Redwing, T. E. Mallouk, *J. Am. Chem. Soc.* **2007**, *129*, 12344–12345.
[109] J. Zhu, Y. Cui, *Nature Mater.* **2010**, *9*, 183–184.
[110] L. Tsakalakow, J. Balch, J. Fronheiser, B. A. Korevaar, *Appl. Phys. Lett.* **2007**, *91*, 233117.
[111] K. Q. Peng, Y. Xu, Y. Wu, Y. J. Yan, S. T. Lee, J. Zhu, *Small* **2005**, *1*, 1062–1067.
[112] T. Stelzner, M. Pietsch, G. Andra, F. Falk, E. Ose, S. Christiansen, *Nanotechnology* **2008**, *19*, 295203.
[113] J. Zhu, Z. Yu, G. F. Burkhard, C. M. Hsu, S. T. Connor, Y. Xu, Q. Wang, M. McGehee, S. Fan, Y. Cui, *Nano Lett.* **2009**, *9*, 279–282.
[114] L. Tsakalakos, J. Balch, J. Fronheiser, M. Y. Shih, S. F. LeBoeuf, M. Pietrzykowski, P. J. Codella, B. A. Korevaar, O. Sulima, J. Rand, A. Davuluru, U. Rapol, *J. Nanophoto.* **2007**, *1*, 013552.
[115] Z. Wu, J. B. Neaton, J. C. Grossman, *Nano Lett.* **2009**, *9*, 2418–2422.
[116] K. Q. Peng, X. Wang, X. L. Wu, S. T. Lee, *Nano Lett.* **2009**, *9*, 3704–3709.
[117] G. Kalita, S. Adhikari, H. R. Aryal, R. Afre, T. Soga, M. Sharon, W. Koichi, M. Umeno. *J. Phys. D* **2009**, *42*, 115104.
[118] S. Y. Lu, Z. Lingley, T. Asano, D. Harris, T. Barwicz, S. Guha, A. Madhukar, *Nano Lett.* **2009**, *9*, 4548–4552.

[119] G. B. Yuan, H. Z. Zhao, X. H. Liu, Z. S. Hasanali, Y. Zou, A. Levine, D. W. Wang, *Angew. Chem.* **2009**, *121*, 9860–9864.
[120] Q. K. Shu, J. Q. Wei, K. L. Wang, H. W. Zhu, Z. Li, Y. Jia, X. C. Gui, N. Guo, X. M. Li, C. R. Ma, D. H. Wu, *Nano Lett.* **2009**, *9*, 4338–4342.
[121] H. Fang, X. D. Li, S. Song, Y. Xu, J. Zhu, *Nanotechnology* **2008**, *19*, 255703.
[122] O. Gunawan, S. Guha, *Sol. Energy Mater. Sol. Cells* **2009**, *93*, 1388–1393.
[123] B. Tian, X. L. Zheng, T. J. Kempa, Y. Fang, N. F. Yu, G. H. Yu, J. L. Huang, C. M. Lieber1, *Nature* **2007**, *449*, 885–889.
[124] B. Tian, T. J. Kempa, C. M. Lieber, *Chem. Soc. Rev.* **2009**, *38*, 16–24.
[125] Y. Cui, C. M. Lieber, *Science* **2001**, *291*, 891–893.
[126] F. Patolsky, G. F. Zheng, C. M. Lieber, *Nanomedicine* **2006**, *1*, 51–65.
[127] F. Patolsky, B. P. Timko, G. H. Yu, Y. Fang, A. B. Greytak, G. F. Zheng, C. M. Lieber, *Science* **2006**, *313*, 1100–1104.
[128] Z. Q. Gao, A. Agarwal, A. D. Trigg, N. Singh, C. Fang, C. H. Tung, Y. Fan, K. D. Buddharaju, J. M. Kong, *Anal. Chem.* **2007**, *79*, 3291–3297.
[129] G. F. Zheng, F. Patolsky, Y. Cui, W. U. Wang, C. M. Lieber, *Nat. Biotechnol.* **2005**, *23*, 1294–1301.
[130] D. K. Nagesha, M. A. Whitehead, J. L. Coffer, *Adv. Mater.* **2005**, *17*, 921–924.
[131] W. Kim, J. K. Ng, M. E. Kunitake, B. R. Conklin, P. D. Yang, *J. Am. Chem. Soc.* **2007**, *129*, 7228–7229.
[132] L. T. Canham, *Adv. Mater.* **1995**, *7*, 1033–1037.
[133] O. Kayser, A. Lemke, N. Hernandez-Trejo, *Curr. Pharm. Biotechnol.* **2005**, *6*, 3–5.
[134] Y. Y. Li, F. Cunin, J. R. Link, T. Gao, R. E. Betts, S. H. Reiver, V. Chin, S. N. Bhatia, M. J. Sailor, *Science* **2003**, *299*, 2045–2047.
[135] E. C. Wu, J.-H. Park, J. Park, E. Segal, F. Cunin, M. J. Sailor, *ACS Nano* **2008**, *2*, 2401–2409.
[136] E. J. Anglin, L. Cheng, W. R. Freeman, M. J. Sailor, *Adv. Drug Delivery Rev.* **2008**, *60*, 1266–1277.
[137] K. S. Brammer, C. Choi, S. Oh, C. J. Cobb, L. S. Connelly, M. Loya, S. D. Kong, S. Jin, *Nano Lett.* **2009**, *9*, 3570–3574.
[138] S. J. Qi, C. Q. Yi, S. L. Ji, C.-C. Fong, M. Yang, *ACS Appl. Mater. Inter.* **2009**, *1*, 30–34.
[139] Y. Jung, L. Tong, A. Tanaudommongkon, J. X. Cheng, C. Yang, *Nano Lett.* **2009**, *9*, 2440–2444.
[140] C. Fang, A. Agarwal, E. Widjaja, M. V. Garland, S. M. Wong, L. Linn, N. M. Khalid, S. M. Salim, N. Balasubramanian, *Chem. Mater.* **2009**, *21*, 3542–3548.
[141] S. Su, Y. He, M. L. Zhang, K. Yang, S. P. Song, X. H. Zhang, C. H. Fan, S. T. Lee, *Appl. Phys. Lett.* **2008**, *93*, 023113.
[142] M. Becker, T. Stelzner, A. Steinbruck, A. Berger, J. Liu, D. Lerose, U. Gosele, S. Christiansen, *ChemPhysChem* **2009**, *10*, 1219–1224.
[143] M. W. Shao, M. L. Zhang, N. B. Wong, D. D. D. Ma, H. Wang, W. W. Chen, S. T. Lee, *Appl. Phys. Lett.* **2008**, *93*, 233118.
[144] B. H. Zhang, H. S. Wang, L. H. Lu, K. L. Ai, G. Zhang, X. L. Cheng, *Adv. Funct. Mater.* **2008**, *18*, 2348–2355.
[145] W. N. Leng, A. A. Yasseri, S. Sharma, Z. Y. Li, H. Y. Woo, D. Vak, G. C. Bazan, A. M. Kelley, *Anal. Chem.* **2006**, *78*, 6279–6282.
[146] E. Galopin, J. Barbillat, Y. Coffinier, S. Szunerits, G. Patriarche, R. Boukherroub, *ACS Appl. Mater. Interf.* **2009**, *1*, 1396–1403.
[147] M. L. Zhang, C. Q. Yi, X. Fan, K. Q. Peng, N. B. Wong, M. S. Yang, R. Q. Zhang, S. T. Lee, *Appl. Phys. Lett.* **2008**, *92*, 043116.
[148] M. L. Zhang, X. Fan, H. W. Zhou, M. W. Shao, J. A. Zapien, N. B. Wong, S. T. Lee, *J. Phys. Chem. C* **2010**, *114*, 1969–1975.
[149] X. T. Wang, W. S. Shi, G. W. She, L. X. Mu, S. T. Lee, *Appl. Phys. Lett.* **2010**, *96*, 053104.
[150] M. W. Shao, L. Lu, H. Wang, S. Z. Luo, D. D. D. Ma, *Microchim. Acta* **2009**, *164*, 157–160.
[151] M. Becker, V. Sivakov, G. Andra, R. Geiger, J. Schreiber, S. Hoffmann, J. Michler, A. P. Milenin, P. Werner, S. H. Christiansen, *Nano Lett.* **2007**, *7*, 75–80.
[152] M. Becker, V. Sivakov, U. Goesele, T. Stelzner, G. Andra, H. J. Reich, S. Hoffmann, J. Michler, S. H. Christiansen, *Small* **2008**, *4*, 398–404.
[153] S. J. Zhuo, M. W. Shao, L. Cheng, R. H. Que, D. D. D. Ma, S. T. Lee, *Appl. Phys. Lett.* **2010**, *96*, 103108.
[154] M. W. Shao, H. Yao, M. L. Zhang, N. B. Wong, Y. Y. Shan, S. T. Lee, *Appl. Phys. Lett.* **2005**, *87*, 183106.
[155] K. Yang, H. Wang, K. Zou, X. H. Zhang, *Nanotechnology* **2006**, *17*, S276–S279.
[156] B. R. Tao, J. Zhang, S. C. Hui, L. J. Wan, *Sens. Actuators, B* **2009**, *142*, 298–303.
[157] X. T. Vu, J. F. Eschermann, R. Stockmann, R. GhoshMoulick, A. Offenhausser, S. Ingebrandt, *Phys. Status Solidi A* **2009**, *206*, 426–434.
[158] W. W. Chen, H. Yao, C. H. Tzang, J. J. Zhu, M. S. Yang, S. T. Lee, *Appl. Phys. Lett.* **2006**, *88*, 213104.
[159] M. W. Shao, Y. Y. Shan, N. B. Wong, S. T. Lee, *Adv. Funct. Mater.* **2005**, *15*, 1478–1482.
[160] Z. H. Chen, J. S. Jie, L. B. Luo, H. Wang, C. S. Lee, S. T. Lee, *Nanotechnology* **2007**, *18*, 345502.
[161] X. T. Zhou, J. Q. Hu, C. P. Li, D. D. D. Ma, C. S. Lee, S. T. Lee, *Chem. Phys. Lett.* **2003**, *369*, 220–224.
[162] L. B. Luo, J. S. Jie, W. F. Zhang, Z. B. He, J. X. Wang, G. D. Yuan, W. J. Zhang, L. C. M. Wu, S. T. Lee, *Appl. Phys. Lett.* **2009**, *94*, 193101.
[163] C. C. Wu, F. H. Ko, Y. S. Yang, D. L. Hsia, B. S. Lee, T. S. Su, *Biosensor. Bioelectron.* **2009**, *25*, 820–825.
[164] L. X. Mu, W. S. Shi, J. C. Chang, S. T. Lee, *Nano Lett.* **2008**, *8*, 104–109.
[165] C. H. Lin, C. H. Hung, C. Y. Hsiao, H. C. Lin, F. H. Ko, Y. S. Yang, *Biosen. Bioelectron.* **2009**, *24*, 3019–3024.
[166] C. Y. Hsiao, C. H. Lin, C. H. Hung, C. J. Su, Y. R. Lo, C. C. Lee, H. C. Lin, F. H. Ko, T. Y. Huang, Y. S. Yang, *Biosen. Bioelectron.* **2009**, *24*, 1223–1229.
[167] D. R. Kim, C. H. Lee, X. L. Zheng, *Nano Lett.* **2009**, *9*, 1984–1988.
[168] K. S. Chang, C. C. Chen, J. T. Sheu, Y. K. Li, *Sens. Actuators, B* **2009**, *138*, 148–153.
[169] X. Y. Bi, W. L. Wong, W. J. Ji, A. Agarwal, N. Balasubramanian, K. L. Yang, *Biosen. Bioelectron.* **2008**, *23*, 1442–1448.
[170] A. Cattani-Scholz, D. Pedone, M. Dubey, S. Neppl, B. Nickel, P. Feulner, J. Schwartz, G. Abstreiter, M. Tornow, *Acs Nano* **2008**, *2*, 1653–1660.
[171] Y. L. Bunimovich, Y. S. Shin, W. S. Yeo, M. Amori, G. Kwong, J. R. Heath, *J. Am. Chem. Soc.* **2006**, *128*, 16323–16331.
[172] L. X. Mu, W. S. Shi, G. W. She, J. C. Chang, S. T. Lee, *Angew. Chem. Int. Ed.* **2009**, *48*, 3469–3472.

Received: June 7, 2010
Published Online: August 16, 2010

